

## NOTES

---

### OBSERVATIONS OF AN INFRARED STAR IN THE ORION NEBULA\*

In January, 1965, an intensity map of the Orion Nebula in the wavelength region from 2.0 to 2.4  $\mu$  was made using a dual-beam photometer optically similar to that described by Westphal, Murray, and Martz (1963), mounted at the Cassegrain focus of the 60-inch telescope at Mount Wilson. In this program 80 per cent of the nebula within a 2' radius of the Trapezium was observed by slowly scanning a 13" aperture in a raster pattern. Detectable radiation was measured throughout the region scanned, with an average measured surface intensity of  $5(\pm 2) \times 10^{-9} \text{ W cm}^{-1} \mu^{-1} \text{ sterad}^{-1}$ , and a maximum intensity of approximately twice the average value. The average measured intensity corresponds to a calculated emission measure of  $3.5 \times 10^6 \text{ cm}^{-6} \text{ pc}$  if it is assumed that all of the radiation is coming from bound-free, free-free, and line hydrogen transitions. A more detailed report on the above observations as well as on further observations at 1.65 and 3.4  $\mu$  is planned for a later paper.

On the survey seven point sources were detected which could be identified positively with photographically visible stars, and one source, whose approximate position is given in Figure 1, was found which could not be identified. During the winter of 1966 photometric observations at  $\lambda\lambda 1.5\text{--}1.8 \mu$ ,  $2.0\text{--}2.4 \mu$ ,  $3.1\text{--}3.8 \mu$ , and  $8.5\text{--}13.5 \mu$  were made of this infrared source using the 24-inch reflector at Mount Wilson and the 200-inch Hale telescope at Mount Palomar. The photometric results are given in Table 1. Figure 2 shows the normalized flux of the infrared object and, for comparison, the energy distribution of a 700° K black body plotted against wavelength. It is seen that the flux at the three longer wavelengths fit a black body quite well, but the flux in the region around 1.65  $\mu$  is low by a factor of 4. The absolute flux calibration was obtained by observing Johnson's (1964, 1965*a*) standard stars.

When considering the nature of this infrared object, it is important to determine whether the object is in front of, behind, or in the nebula.

If the object is in front of the nebula, it must be an extremely cool star, comparable to the coolest found in the California Institute of Technology Infrared Sky Survey (Neugebauer, Martz, and Leighton 1965; Ulrich, Neugebauer, McCammon, Leighton, Hughes, and Becklin 1966). The probability of finding such an infrared star just coinciding with the nebula is very small, and this possibility will not be discussed further.

If the object is behind the nebula, it might be an ordinary type of star that is extremely reddened. An upper limit to the probability of such a star being situated behind the nebula can be made by considering the area scanned and the surface density near the galactic plane of stars whose apparent magnitude at 10  $\mu$  is brighter than  $-1.2$ —the apparent magnitude of the object. From the work of Low and Johnson (1964), Johnson (1964), and Barnhart and Mitchell (1966) it is estimated that the number of such stars near the galactic plane is less than 100, which leads directly to a surface density less than  $10^{-5}$  per sq. min of arc. The area scanned was about 10 sq. min of arc, so the a priori probability of the object being an ordinary star is less than  $10^{-4}$ . If the object is a common type of star, the apparent magnitude of  $-1.2$  at 10  $\mu$  and the minimum distance modulus of 8.5 (Markowitz 1948; Sharpless 1952; Strand 1958) requires that it be a red supergiant. If, in fact, the object is a red supergiant, extrapolation of a typical absorption curve

\* Supported in part by National Aeronautics and Space Administration grant NsG-426.



FIG. 1.—Finding chart

(Johnson and Borgman 1963) shows that the total amount of absorption in the visible would be about 35 mag.

When we consider the small a priori probability of finding a common type of star in the region scanned, together with the enormous absorption that would be required, we are led to conclude that the object is probably located inside the nebula itself.

There is, in fact, some independent observational evidence that the source may be located in the nebula. Although spatial scans at the east-arm Cassegrain focus of the 200-inch telescope using a 6" aperture indicate that the object is a point source to within 2" at both  $\lambda 2.2$  and  $\lambda 10 \mu$ , broad wings extend 30" from the source. This is shown by

TABLE 1  
PHOTOMETRIC RESULTS

Effective Wavelength ( $\mu$ )	Wave-length Pass Band ( $\mu$ )	Magnitude	Absolute Flux ( $W \text{ cm}^{-2} \mu^{-1}$ ) $\times 10^{16}$
1 65	0 3	9 8	0 14 $\pm$ 0 03
2 2	0 4	5 2	3 4 $\pm$ 2
3 4	0 7	2 0	13 2 $\pm$ 8
10 0	5 0	-1 2	3 4 $\pm$ 0 3

TABLE 2  
CORRECTED FLUXES AND INFERRED PARAMETERS

OPTICAL DEPTH IN VISIBLE	CORRECTED FLUX ( $W \text{ cm}^{-2} \mu^{-1} \times 10^{17}$ )				THREE-COLOR TEMPERATURE ( $^{\circ} \text{K}$ )	BOLOMETRIC MAGNITUDE	RADIUS (a u)
	1 65 $\mu$	2 2 $\mu$	3.4 $\mu$	10 $\mu$			
0	1 4	34	132	34	700	-1 9	8
2 5	2 6	52	153	35	725	-2 0	8
5 0	5	79	177	36	760	-2 4	8
10 0	18	175	240	38	900	-3 0	6
15 0	65	400	320	40	1100	-3 9	6

the fact that within 30" east and west of the source the average intensity at 2.2  $\mu$  is 12.0 ( $\pm 0.5$ )  $\times 10^{-9} W \text{ cm}^{-2} \mu^{-1} \text{sterad}^{-1}$ , while between 30" and 50" away from the source the average intensity is 7.0 ( $\pm 0.5$ )  $\times 10^{-9} W \text{ cm}^{-2} \mu^{-1} \text{sterad}^{-1}$ . Wings were not observed on any stars outside the nebula. The chance that the central core is accidentally associated with these wings is small since in the 10 sq. min of arc area scanned the only other region found with a similar increase in flux was centered around the Trapezium. The probability that the coincidence is accidental is thus less than 0.1.

A correction for nebular absorption has been calculated for several amounts of total absorption typically expected in the nebula. A three-color temperature ( $\lambda \lambda 2.2, 3.4, 10 \mu$ ) of a source necessary to give the observed flux has been derived using an absorption curve, shown in Figure 3, obtained from the data of Johnson and Borgman (1963), Johnson (1965*b*), and infrared measurements of  $\theta^1$  (C) Orionis. Table 2 presents the results of these calculations, plus an approximate bolometric magnitude and a calculated radius assuming the object is at a distance of 500 pc (Markowitz 1948; Sharpless 1952; Strand 1958). The Trapezium has a visual absorption of less than 3 mag (Johnson 1965*b*);

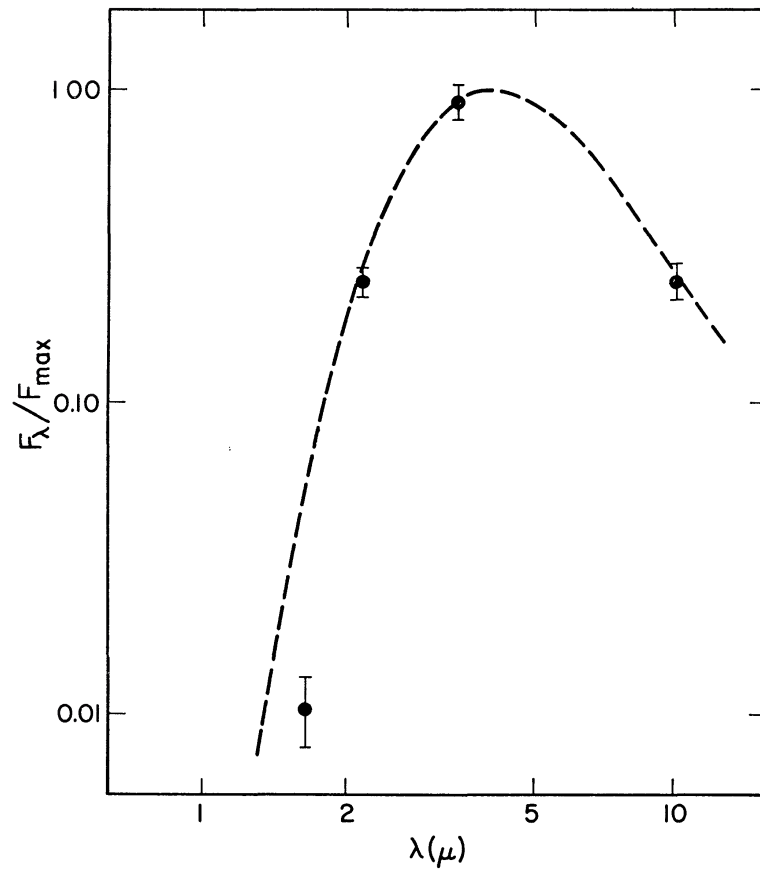


FIG. 2.—Normalized flux versus wavelength and, for comparison, a 700° K black body

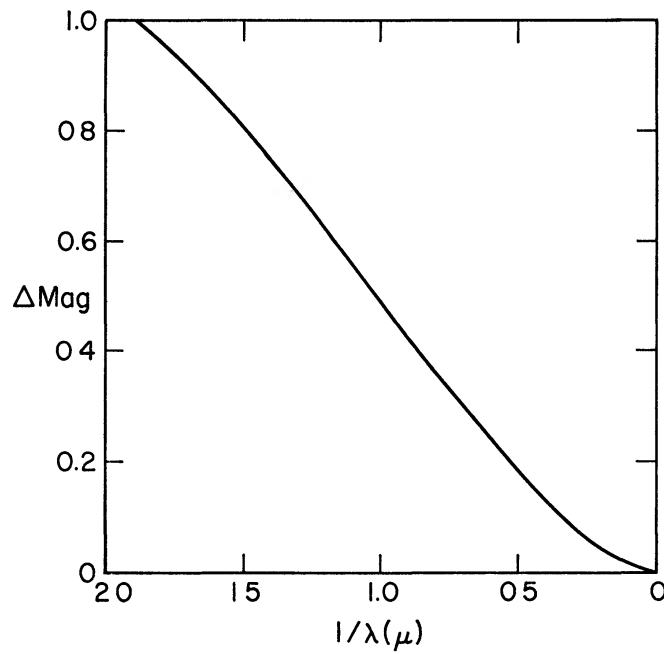


FIG. 3.—Absorption curve for the Orion Nebula

yet even if 5 times this optical depth is considered ( $\tau_v \sim 15$ ) the energy distribution still requires a rather low source temperature, less than  $1200^\circ \text{K}$ .

From the above discussion we feel that the object is in the nebula and has a gravitationally associated cool shell. It is well known that the Orion Nebula is a very young association and that the probability of finding a star in the process of forming should be relatively high (Aller and Liller 1959). Thus an attractive interpretation of the observations is that the infrared object is a protostar. If the star has a radius  $R$  of 8 a.u., a temperature  $T$  of  $700^\circ \text{K}$ , and a mass  $M$  of  $6 M_\odot$ , the Kelvin time scale,

$$\tau = \frac{GM^2}{4\pi R^3 \sigma T^4},$$

is  $10^3$  years. This number is probably consistent with the approximate age of the Orion Nebula  $2 \times 10^4$  years established by Vandervoort (1964) or the Trapezium expansion age of  $< 10^4$  years given by Parenago (1953).

We would like to thank all those associated with the California Institute of Technology's Infrared Sky Survey for their assistance. A special thanks goes to J. Westphal for making the  $10\text{-}\mu$  observations, Drs. R. B. Leighton and G. Münch for helpful advice, and D. Martz for construction and design of the photometer.

E. E. BECKLIN  
G. NEUGEBAUER

September 12, 1966

CALIFORNIA INSTITUTE OF TECHNOLOGY  
PASADENA, CALIFORNIA

#### REFERENCES

- Aller, L. H., and Liller, W. 1959, *Ap. J.*, **130**, 45.  
 Barnhart, P. E., and Mitchell, W. E. 1966, *Contributions from the Perkins Observatory*, Ser. II, No. 16.  
 Johnson, H. L. 1964, *Bol. Tonantzínula y Tacubaya Obs.*, **3**, 305.  
 ———. 1965a, *Com. Lunar and Planetary Lab.*, No. 53.  
 ———. 1965b, *Ap. J.*, **141**, 923.  
 Johnson, H. L., and Borgman, J. 1963, *B.A.N.*, **17**, 115.  
 Low, F. J., and Johnson, H. L. 1964, *Ap. J.*, **139**, 1130.  
 Markowitz, W. M. 1948, *A.J.*, **54**, 111.  
 Neugebauer, G., Martz, D. E., and Leighton, R. B. 1965, *Ap. J.*, **142**, 399.  
 Parenago, P. P. 1953, *Astr. Zh.*, **30**, 249.  
 Sharpless, S. 1952, *Ap. J.*, **116**, 251.  
 Strand, K. 1958, *Ap. J.*, **128**, 14.  
 Ulrich, B., Neugebauer, G., McCammon, D., Leighton, R. B., Hughes, E. E., and Becklin, E. 1966, *Ap. J.*, **146**, 288.  
 Vandervoort, P. O. 1964, *Ap. J.*, **139**, 869.  
 Westphal, J. A., Murray, B. C., and Martz, D. E. 1963, *Appl. Opt.*, **2**, 749.

## VARIABILITY OF INFRARED STARS

### I. LONG-PERIOD VARIABLES

In a recent paper Wing, Spinrad, and Kuhl (1966) have found that of three infrared objects observed by Neugebauer, Martz, and Leighton (1965) two are Mira-type variables, with exceedingly long periods. Similarly Ulrich, Neugebauer, McCammon, Leighton, Hughes, and Becklin (1966) have found that five of the fourteen newly discovered infrared stars are known Mira-type variables, with periods greater than  $400^d$ .

These investigations suggested a re-examination, from this point of view, of the re-

sults obtained in the near infrared using the telescopes of Asiago and Loiano (Maffei 1963*b*, 1966*b*). The investigations have led to the discovery of fifteen variables, which, according to their light-curves, were assigned as Mira-type variables. These stars were discovered in three fields centered on M20, M17, and in Monoceros at  $\alpha = 6^{\text{h}}31^{\text{m}}4^{\text{s}}$ ;  $\delta = +9^{\circ}30'$  (1900.0). The first two fields are 1 square degree each while the third is of 28 square degrees. The infrared magnitude limit was about 16.0–16.5 in the M20 and M17 fields and 14.0 in the Monoceros field. The near-infrared region between 6800 and 8800 Å was observed using a combination of Eastman I-N hypersensitized plates and an RG 5 filter.

In Table 1 we list the variables assigned to the Mira type. The numeration is that adopted in the original papers; these papers contain also the identification charts and additional details.

TABLE 1  
POSITIONS, INFRARED MAGNITUDES, PERIODS, AND EPOCHS OF THE RECENTLY  
DISCOVERED VARIABLES ASSIGNED TO THE MIRA TYPE

No	$\alpha(1900)$	$\delta(1900)$	$m_{\text{ir}}$	Period	Epoch gg 243
M20:					
2	17 <sup>h</sup> 56 <sup>m</sup> 35 <sup>s</sup>	−23°21'9	7 0–14 2	400 <sup>d</sup> ::	6454
5	57 26	−22 59 8	8 3–14 8	510	7180
6	55 26	−22 57 2	11 6–14 4	408	7843
9	55 58	−23 33 1	9 0–13 3	440::	6705:
M17:					
1	18 12 55	−15 58 0	13 4–16 4	550::	7547
4	15 13	−15 55 6	12 3–15 3	250	7585
5	15 20	−16 22 1	14 9–16 4	430::	7479:
6	15 40	−16 19 8	13 9–16 0	270	7875
7	15 48	−16 16 2	13 1–15 5	385	7435
10	16 35	−16 31 1	11 8–16 2	520:	7841
11	16 37	−16 20 0	9 5–14 6	467	7875
Mon:					
2.	6 24 08	+ 8 48 1	9 5–13 6	820::	7360::
3	28 59	+11 09 5	12 0–13 6	234	6957
5.	34 23	+ 7 23 3	8 9–11 8	328	7380
6	39 26	+ 9 56 4	9 2–10 9	355	7560

In the *General Catalogue of Variable Stars*, only two Mira-type variables are present in the fields mentioned; these are RZ and FX Mon. This fact shows that the number of Mira-type variables increases markedly when infrared observations are used.

From Table 1 it follows also that nine of the fifteen stars have very long periods ( $\geq 400^{\text{d}}$ ). On the other hand, in the *General Catalogue*, which is mainly based on photographic and photovisual observations, these long-period stars ( $P \geq 400^{\text{d}}$ ) make up only 7.7 per cent of the total.

It should be noticed that the probability of discovery is lower for infrared Mira stars, because of the longer periods and the smaller amplitude of variation in the infrared. The last difficulty is greatly reduced with the technique used in our investigations, while it was serious in Hetzler's observations (1937) because no TiO bands occur in the wavelength range used by him for spectra not later than M5. In other words, these observations, made with a longer base line than those of Hetzler, show that the amplitudes of the long-period variables tend to be as large in the infrared as in blue wavelengths.

Further investigations of the variability of infrared stars may prove of great importance: indeed, a confirmation of these results would imply that the very long-period Mira stars are by far the most abundant ones.

## II. T TAU VARIABLES

Following Mendoza V. (1966) the energy distribution in the visible-infrared for some T Tau stars requires a complex model involving either duplicity or a large envelope.

The same two causes may explain the differences in behavior, in the blue and infrared regions, suspected for certain T Tau variables, in the vicinity of NGC 1999 (Maffei 1963a).

Very recently (Maffei 1966a), a remarkable difference between blue-infrared behavior was detected for VY Mon. While the infrared observations of this T Tau type variable show slow variations, in blue light the star remains for the most part constant and at minimum light; at maximum phase irregular variations in blue light have been noted. This star requires further observations.

PAOLO MAFFEI

September 12, 1966; revised October 11, 1966

LABORATORIO DI ASTROFISICA DELLA  
UNIVERSITÀ DI ROMA

## REFERENCES

- Hetzler, C. 1937, *Ap. J.*, **83**, 372.  
 Maffei, P. 1963a, *Mem. Soc. Astr. Italiana*, **34**, 57.  
 ———. 1963b, *ibid.*, p. 441.  
 ———. 1966a, *ibid.*, **37**, 459.  
 ———. 1966b, *ibid.*, p. 475.  
 Mendoza V., E. E. 1966, *Ap. J.*, **143**, 1010.  
 Neugebauer, G., Martz, D. E., and Leighton, R. B. 1965, *Ap. J.*, **142**, 399.  
 Wing, R. F., Spinrad, H., and Kuhl, L. V. 1966, *Ap. J.*, **147**, 117.  
 Ulrich, B. T., Neugebauer, G., McCammon, D., Leighton, R. B., Hughes, E. E., and Becklin, E. 1966, *Ap. J.*, **146**, 288.

---

THE WIDTH OF THE NULL LINE  $\lambda 4065$  OF Fe I IN THE  
SPECTRUM OF BETA CORONAE BOREALIS\*

It was noted recently (Preston and Sturch 1966) that, because the  $z^5F_1^o-g^5D_0$  transition  $\lambda 4065.40$  of Fe I is unaffected by the presence of a magnetic field, its width may be used to estimate the broadening due to axial rotation in sharp-lined magnetic stars. From a comparison of the half-half width of this line in  $\beta$  CrB, derived from 2 Å/mm spectrograms, with the equatorial rotational velocity inferred on the oblique-rotator model from the magnetic period of 18.5 days, Preston and Sturch obtained an inclination of the rotation axis to the line of sight  $i = 30^\circ$  if turbulent broadening is negligible. This result can be criticized in two ways: (1) higher spectroscopic resolution is desirable because the observed width of  $\lambda 4065$  barely exceeds the projected slit width at the dispersion used by Preston and Sturch, and (2) the conversion of line width to  $v_{\text{rot}} \sin i$  did not take rotational broadening into account properly and ignored limb darkening altogether. We attempt to meet these objections in this Note.

Two 1.3 Å/mm spectrograms of  $\beta$  CrB were obtained in 1966 in the third order of a 600 groove/mm Babcock grating with the 160-inch camera of the 120-inch coude spectrograph. Mean profiles of Fe I  $\lambda 4065$  and several weak Fe I comparison lines were derived from direct-intensity microphotometer tracings of the  $\lambda 4065$  region reproduced in Figure 1. An iterative unsmearing process was used to obtain an intrinsic stellar profile which, when folded with the instrumental profile, resulted in a profile that differed from the observed profile by less than 2 per cent at all wavelengths. Comparison of the instrumental and intrinsic stellar profiles shown in Figure 2 shows that, while the stellar line

\* *Contributions from the Lick Observatory*, No. 219.

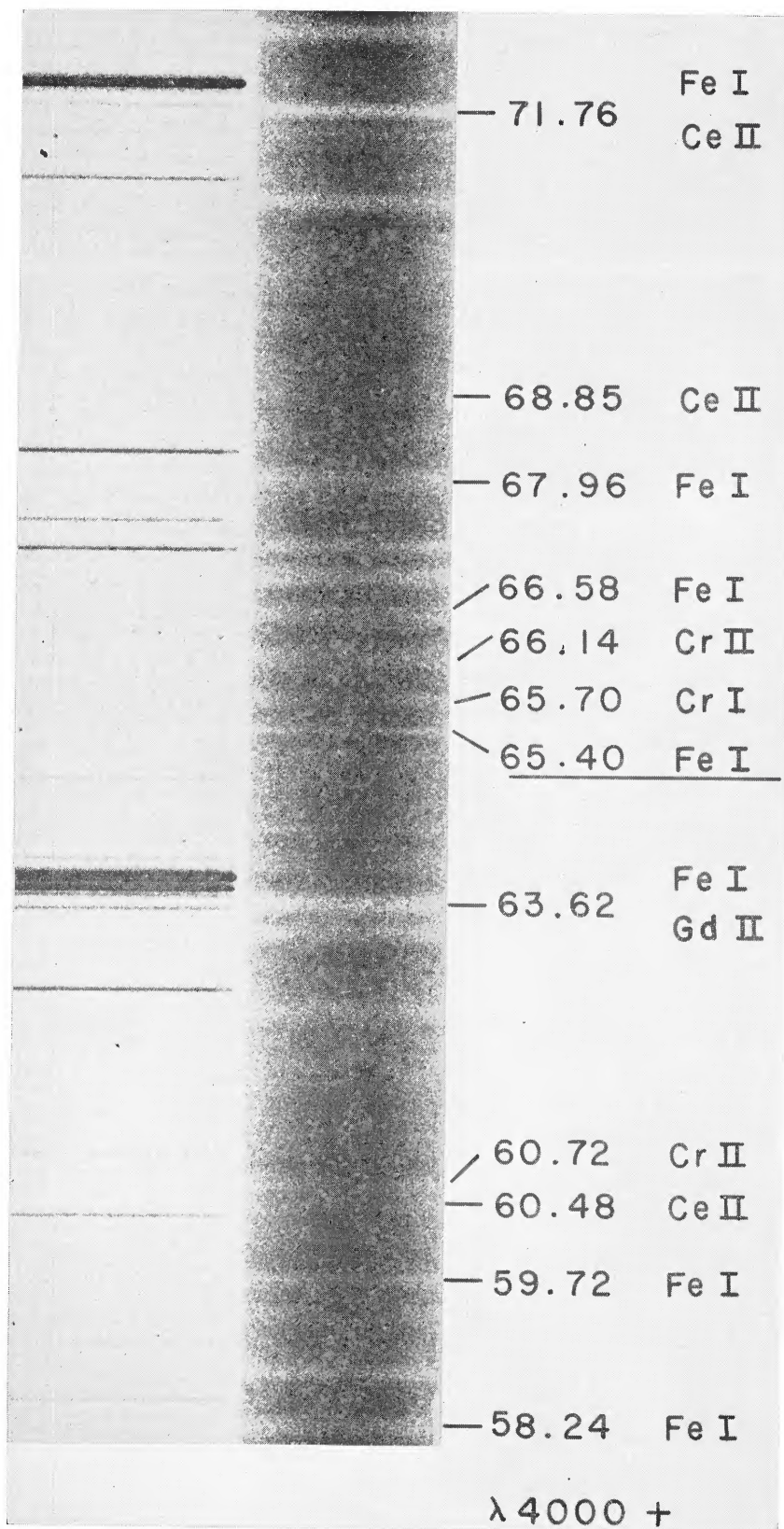


FIG. 1.—Reproduction of the spectral region near the null line Fe I  $\lambda 4065$  in  $\beta$  CrB. The null line is noticeably narrower than the neighboring absorption features, all of which are broadened by the Zeeman effect. The identifications are those of Hiltner (1945). Unmarked lines are either blends or were unidentified by Hiltner. The original dispersion was  $1.3 \text{ \AA}/\text{mm}$ .

width clearly exceeds the instrumental width, the line is nevertheless so narrow that it is probably unwise to base conclusions on either the shape of the core or of the wings which are lost in a complicated background of other absorption lines. Therefore, we characterize the shape of the line by its half-half width for which we obtain  $w_{1/2} = 2.5$  km/sec, slightly less than the value of 3.0 km/sec obtained by Preston and Sturch. An adjustment of 10 per cent in the adopted height of the reference continuum produces a change in  $w_{1/2}$  of 0.3 km/sec.

We infer the projected rotational velocity of  $\beta$  CrB from  $w_{1/2}$  as follows. We assume that weak lines produced by an area element of the stellar disk have Gaussian profiles characterized by a local atmospheric Doppler parameter

$$v_l = (v_T^2 + v_t^2)^{1/2},$$

where  $v_T$  and  $v_t$  are the thermal and turbulent Doppler parameters, respectively. These profiles were then rotationally broadened by means of Unsöld's (1938) rotational-broadening function. A limb-darkening coefficient  $\beta = 1.5$  was adopted. Rotational profiles due to projected rotational velocities of  $v_{\text{rot}} \sin i = 2, 4,$  and  $6$  km/sec were calculated for the cases (a)  $v_T = 1.5$  km/sec (for Fe at  $T = 8000^\circ$  K) with  $v_t = 0$ , and

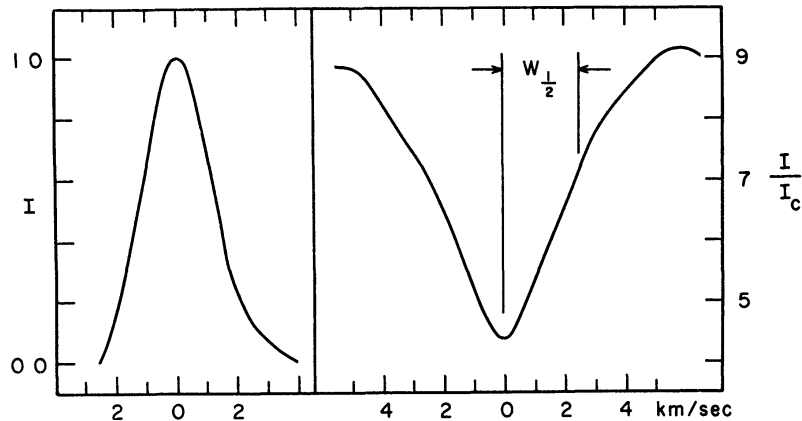


FIG. 2.—Intensity profiles. (a) The instrumental profile derived from weak Fe I comparison lines; (b) the profile of Fe I  $\lambda 4065$  corrected for instrumental broadening. Intensities in (b) are in units of the continuum intensities  $I_c$ .

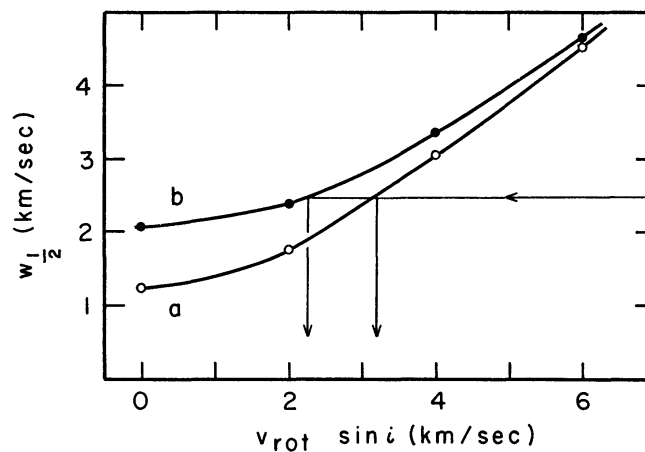


FIG. 3—Relations between the half-half width  $w_{1/2}$  and  $v_{\text{rot}} \sin i$  for two values of the local atmospheric Doppler parameter: (a)  $v_l = 1.5$  km/sec and (b)  $v_l = 2.5$  km/sec as described in the text.

(b)  $v_T = 1.5$  km/sec with  $v_t = 2.0$  km/sec. The values of  $w_{1/2}$  obtained from these profiles are plotted versus  $v_{\text{rot}} \sin i$  in Figure 3. Entering Figure 3 with  $w_{1/2} = 2.5$  km/sec, we obtain for  $\beta$  CrB  $v_{\text{rot}} \sin i = 3.2$  km/sec for case (a) and 2.3 km/sec for case (b). The former value may be taken to be an upper limit that corresponds to no atmospheric turbulence. Comparison of the results from cases (a) and (b) indicates the extent to which the result depends on the presence of turbulence. It should be noted that this upper limit will be too large if broadening due to damping cannot be neglected for  $\lambda 4065$  in  $\beta$  CrB. The empirical correction for this effect by Preston and Sturch led to  $v_t = 2.2$  km/sec, or  $v_t = 1.5$  km/sec if  $v_T = 1.5$  km/sec. These parameters correspond to a case intermediate between cases (a) and (b) and lead to  $v_{\text{rot}} \sin i = 2.7$  km/sec. Thus, when limb darkening, rotational broadening, and damping are all taken into account, it appears that  $v_{\text{rot}} \sin i < 3$  km/sec, an upper limit somewhat greater than the value of 2 km/sec given by Preston and Sturch.

According to the oblique-rotator model the period of 18.5 days corresponds to  $v_{\text{rot}} \approx 6$  km/sec, so that  $i < 30^\circ$ . For a dipole field the observed ratio of the maximum and minimum effective magnetic fields  $H_e(\text{max})/H_e(\text{min}) = -1.4$  then implies that the axis of symmetry of the dipole is inclined by no more than  $6^\circ$  to the rotational equatorial plane. It remains to be seen whether or not this condition can be relaxed by the assumption of another field geometry.

GEORGE W. PRESTON

August 2, 1966  
LICK OBSERVATORY  
UNIVERSITY OF CALIFORNIA  
MOUNT HAMILTON, CALIFORNIA

#### REFERENCES

- Hiltner, W. A. 1945, *Ap. J.*, **102**, 438.  
Preston, G. W., and Sturch, C. 1966, *Proc. A.A.S.-N.A.S.A. Symp. on Peculiar A-Type Stars* (in press).  
Unsöld, A. 1938, *Physik der Sternatmosphären* (Berlin: Springer-Verlag), p. 318.

#### ABSORPTION LINES IN NEUTRON-STAR SPECTRA

Neutron stars have been proposed as one possible explanation for the strong X-ray sources discovered in recent rocket flights. Morton (1964) computed gray model atmospheres for such objects, and Orszag (1965) computed the continuous spectra in several cases, taking into account possible absorption edges. Orszag's calculations predict the existence of sharp discontinuities in the spectra of the cooler models, which would distinguish neutron stars from other possible X-ray sources. However, in the spectra of many classes of stars, for example, in the ultraviolet spectra of B stars (Morton 1965), strong absorption lines also modify the continuous spectrum considerably. It is the purpose of this Note to estimate the importance of absorption lines in the spectra of neutron stars.

We have used the theoretical curve of growth based on a Schuster-Schwarzschild model atmosphere, for which the limiting expressions for the equivalent width in the linear, logarithmic, and damping regions are

$$\frac{W_\lambda}{\lambda} = \pi^{1/2} X_0 \frac{v_0}{c}, \quad \frac{W_\lambda}{\lambda} = \frac{2 v_0}{c} \sqrt{(\ln X_0)}, \quad \text{and} \quad \frac{W_\lambda}{\lambda} = \frac{\pi^{1/4}}{2} \sqrt{\left(\frac{X_0 v_0 \gamma \lambda}{c^2}\right)}, \quad (1)$$

respectively, where  $X_0 = (\pi^{1/2} e^2 N f \lambda) / (m c v_0)$ ,  $v_0 = (2kT/M)^{1/2}$  is the average thermal velocity of the absorbing ion,  $N$  is the number of absorbing ions above the photosphere,  $f$  is the oscillator strength, and  $\gamma$  is the effective damping constant (Ambartsumian 1958).

We adopt the composition assumed by Orszag (carbon, 35 per cent; nitrogen, 5 per cent; oxygen, 55 per cent; neon, 5 per cent), and we consider two combinations of temperature and density:

$$\text{Case A: } T = 10^7 \text{ }^\circ\text{K}, \quad \rho = 0.2 \text{ gm/cm}^3;$$

$$\text{Case B: } T = 5 \times 10^6 \text{ }^\circ\text{K}, \quad \rho = 0.6 \text{ gm/cm}^3.$$

These values correspond to the temperature and density at optical depth  $\frac{2}{3}$  in Morton's models. We take the value  $g = 2 \times 10^{14} \text{ cm/sec}^2$  in both cases.

TABLE 1  
PROPERTIES OF IONS IN NEUTRON-STAR ATMOSPHERES

ELEMENT	ABUN- DANCE (Per Cent)	PERCENTAGE OF IONS WITH ONE BOUND ELECTRON		NUMBER OF GROUND-STATE IONS ABOVE THE PHOTOSPHERE	
		Case A	Case B	Case A	Case B
Carbon	35	0 1	1 2	$4.6 \times 10^{18}$	$1.1 \times 10^{20}$
Nitrogen	5	1	1 7	$8.1 \times 10^{17}$	$2.0 \times 10^{19}$
Oxygen	55	2	2 6	$9.6 \times 10^{18}$	$3.1 \times 10^{20}$
Neon	5	0 2	7 1	$1.2 \times 10^{18}$	$6.4 \times 10^{19}$

TABLE 2  
EQUIVALENT WIDTHS OF O VIII LINES

LINE	WAVE- LENGTH (Å)	EQUIVALENT WIDTH (Å) (NATURAL BROADENING)		EQUIVALENT WIDTH (Å) (STARK BROADENING)	
		Case A	Case B	Case A	Case B
Ly- $\alpha$	19 00	0 03	0 15	0 6	6
Ly- $\beta$	16 03	02	02	5	5
Ly- $\gamma$	15 20	02	02	5	5
Ly- $\delta$	14 84	02	02	5	5
Ly- $\epsilon$	14 66	0 02	0 02	0 6	6

At these high temperatures, the elements are almost completely ionized, and absorption lines can be produced only by the few remaining one-electron ions. The fractions of ions with one bound electron, computed from the Saha equation, are shown in Table 1. The calculation of the partition functions included the effect of perturbations by neighboring particles by using the asymptotic expression for the occupation probability  $W_n$ ,

$$\log W_n = 14.69 - \frac{2}{3} \log N + \log Z - 4 \log n, \quad (2)$$

given by de Jager and Neven (1960), where  $N$  is the density of the perturbing particles,  $n$  is the quantum number of the state, and  $Z$  is the atomic number of the perturbed ion. The effective depth of the reversing layer,  $H = P/g\rho$ , is 2.1 cm in Case A and 1.0 cm in Case B. The numbers of ground-state ions above the photosphere are also given in Table 1. We see that oxygen has the largest number of absorbing ions above the photosphere in each case, and so we shall restrict ourselves to consideration of the resonance lines of this ion.

We first compute the equivalent widths under the assumption that radiative damping is the only important broadening mechanism. Since we are dealing with a one-electron atom, we can use the  $gf$ -values of hydrogen directly. However, the radiative damping constant,  $\gamma_n = \sum_m A_{nm}$ , will be higher than that for hydrogen, since the Einstein transition probability  $A_{nm}$  is proportional to  $1/\lambda^2$ . The third and fourth columns of Table 2 contain the equivalent widths of the first five lines of the Lyman series of O VIII. All of these lines, except Ly- $\alpha$  and Ly- $\beta$  in Case B, fall on the logarithmic part of the curve of growth, and therefore are not very sensitive to the assumed abundances. We see that in both cases the widths are small compared to the spacing between the lines. Therefore, if radiative damping were the only important broadening mechanism, the lines would not have any appreciable effect on the continuous spectrum.

However, Stark broadening probably has a marked effect on these lines, increasing the effective damping constant above the radiative value. Stark profiles have not been calculated for very high densities and temperatures, but the asymptotic formula given by Griem (1960, eq. [29]) can be used to obtain an estimate for the effective damping constant. Equivalent widths computed with damping constants obtained from Griem's formula are given in the last two columns of Table 2. In both cases the equivalent widths are large compared to the spacing between the lines. We conclude therefore that Stark-broadened absorption lines will considerably modify the continuous spectrum. In particular, the absorption edges predicted by Orszag will likely be completely obliterated and so will not be a distinguishing characteristic of neutron-star spectra. Clearly, the effect of line absorption should be taken into account in future calculations of neutron-star atmospheres.

P. E. ONYEJUBA  
J. E. GAUSTAD

June 13, 1966; revised July 22, 1966

DEPARTMENT OF MATHEMATICS AND STATISTICS  
UNIVERSITY OF NIGERIA  
NSUKKA, NIGERIA

#### REFERENCES

- Ambartsumian, V. A. 1958, *Theoretical Astrophysics* (New York: Pergamon Press), pp. 152 ff.  
Griem, H. R. 1960, *A p. J.*, **132**, 883.  
Jager, C. de, and Neven, L. 1960, *B.A.N.*, **15**, 55.  
Morton, D. C. 1964, *A p. J.*, **140**, 460.  
———. 1965, *ibid.*, **141**, 73.  
Orszag, S. A. 1965, *A p. J.*, **142**, 473.

---

#### PROBLEMS RELATING TO MAGNETIC FIELDS IN NEUTRON STARS

Within the last few years a number of papers on X-ray emission from neutron star magnetospheres have been published (Cameron 1965*a, b*; Tsuruta and Cameron 1966; Friedman, Byram, and Chubb 1966; Surdin 1966). All these papers hinge on the suggestion (Woltjer 1964) that the magnetic field in a neutron star may be as large as  $10^{14}$ – $10^{16}$  gauss. In this communication we point out certain consequences of Woltjer's suggestion which militate strongly against the viability of the proposed magnetic neutron star configurations.

To begin with, as pointed out by Landau and Lifshitz (1959), magnetic fields in excess of about  $6 \times 10^{15}$  gauss lead to internal inconsistencies within classical electrodynamics. In other words, such fields and their interactions with classical electrons are not describable by Maxwell's equations and Lorentz forces, and hence such interactions are as yet undefined.

As pointed out further by Landau and Lifshitz, a considerably lower limit than that due to classical theory is imposed by quantum effects at  $\sim 2 \times 10^{14}$  gauss. In such a field there are two distinct effects peculiar to quantum mechanics which can take place. First an electron with its spin antiparallel to the field has, apart from its rest mass, an energy of  $2 m_0 c^2$ . Therefore, upon transition to the ground state (spin aligned with the field), a positron-electron pair may be created. Second, because the transverse motion of charged particles in magnetic fields is quantized, an electron in a circular orbit ( $n = 1$ ) with its spin aligned with the field has also an energy of  $2 m_0 c^2$  in excess of its rest energy. Again, upon transition to the ground state ( $n = 0$ ), a positron-electron pair may be created. Thus it appears that in the strong field particle numbers are not conserved and quantum field effects must be very pronounced.

Let us pursue this line of thought a little further, for in neutron stars rather peculiar effects may occur in fields already much weaker than the critical field of  $2 \times 10^{14}$  gauss. These effects arise because electrons in the magnetic field have an energy distribution defined by the thermostat in the form of the boundaries of the system: for a neutron star this would be the interior as well as the surface temperature of the star. Thus, for example, no transverse electron motion is possible in a magnetic field in excess of  $10^{11}$  gauss if the temperature is below  $10^7$  ° K. Obviously, under these conditions the motion of the electrons is restricted to trajectories along the field lines and therefore, locally, the electron gas behaves nearly like a one-dimensional gas.

Since the phase space of such a gas is much smaller than that for a three-dimensional gas, degeneracy will set in at an earlier stage of collapse. It is not clear how this will affect the detailed structure of the neutron star. However, it seems likely that the object will tend to expand along the magnetic field lines into a sausage-like configuration, quite remote from the nearly spherical symmetry studied hitherto. Such a deformation may be viewed as an extreme case of an instability due to the anisotropy in thermal conductivity of degenerate electron gas in a magnetic field (Wyller 1964).

In addition, it seems that the opacity of the magnetic neutron star will be highly anisotropic—the object being nearly transparent along the magnetic field. This is because the electrons are constrained to move along the field lines and thus cannot scatter photons with energies below several kilo electron volts. This will obviously affect adversely the stability as well as the lifetime of the configuration.

Recently Woltjer (1966) has suggested that the effects of anisotropy might be considerably diminished if the high-intensity portion of the field is confined within the collapsed objects, i.e., if most of the field lines close inside the body. It is not clear how such a configuration would result within the context of the theory upon which the high magnetic field in neutron stars is predicated. However, granting the possibility of such an end state of collapse, it is evident that the magnetosphere associated with this object will be, relatively speaking, insignificant.

The author wishes to acknowledge the critical discussions with J. W. Carpenter of American Science and Engineering as well as the exchanges with L. Woltjer of Columbia University.

OSCAR P. MANLEY

September 8, 1966; revised October 24, 1966  
 AMERICAN SCIENCE AND ENGINEERING, INC.  
 CAMBRIDGE, MASSACHUSETTS

#### REFERENCES

- Cameron, A. G. W. 1965a, *Nature*, **205**, 787.  
 ———. 1965b, *ibid*, **206**, 1342  
 Friedman, H., Byram, E. T., and Chubb, T. A. 1966, *Science* (preprint).  
 Landau, L. D., and Lifshitz, E. M. 1959, *The Classical Theory of Fields* (Reading, Mass.: Addison-Wesley Publishing Co.).

- Surdin, M. 1966, *Nature*, **209**, 5018.  
 Tsuruta, S., and Cameron, A. G. W. 1966, *Nature*, **211**, 5047.  
 Woltjer, L. 1964, *Ap. J.*, **140**, 1309.  
 ———. 1966, private communication.  
 Wyller, A. 1964 *Ap. Norv.*, **9**, No. 9.

---

### ON THE LIMB DARKENING OF PLANETARY ATMOSPHERES IN THE THERMAL INFRARED

Thermal maps of Venus (Murray, Wildey, and Westphal 1963; Westphal, Wildey, and Murray 1965) and Jupiter (Murray *et al.* 1964) have demonstrated that limb darkening in the 8–14-micron wavelength interval is pronounced for these two planets. Since both these planets are completely cloud-covered, it is possible that both anisotropic multiple scattering (Goody 1964) and a temperature gradient (Pollack and Sagan 1965) are responsible. It is the purpose of this Note to demonstrate how exact solutions to the *standard* problem—that of describing the angular distribution of outgoing radiation from a slab of material bounded on both sides by a vacuum (Chandrasekhar 1950)—may be expressed in terms of Chandrasekhar's  $\psi$ - and  $\phi$ -functions of zero order when both scattering and temperature-gradient effects are present. The additional problem of imposing the correct lower boundary conditions to account for surface effects in order to specify the angular distribution of outgoing thermal radiation (limb darkening) from the atmosphere is quite straightforward (cf. Chandrasekhar 1950, pp. 269–274) and will not be presented here.

Let  $I_P(\tau, \mu)$  be the monochromatic specific intensity of thermal radiation in a doubly infinite plane-parallel atmosphere. Consider an atmosphere of finite thickness  $\tau_1 = \tau_3 - \tau_2$  having scattering and thermal emission properties identical with those that the doubly infinite atmosphere has in the range ( $\tau_2 \leq \tau \leq \tau_3$ ). Let  $I(0, +\mu)$  and  $I(\tau_1, -\mu)$  designate the outgoing radiation fields in the directions  $+\mu$  and  $-\mu$  ( $0 < \mu \leq 1$ ) at the levels  $\tau = 0$  and  $\tau = \tau_1$ , respectively.

By developing an invariance principle similar to Chandrasekhar's (1950) (see also Mullikin 1962) it is found that the solutions for the standard problem are given by

$$\begin{aligned}
 I(0, +\mu) = I_P(0, +\mu) - \frac{1}{2\mu} \int_0^1 S(\tau_1; \mu, \mu') I_P(0, -\mu') d\mu' \\
 - e^{-\tau_1/\mu} I_P(\tau_1, +\mu) - \frac{1}{2\mu} \int_0^1 T(\tau_1; \mu, \mu') I_P(\tau_1, +\mu') d\mu'
 \end{aligned} \tag{1}$$

and

$$\begin{aligned}
 I(\tau_1, -\mu) = I_P(\tau_1, -\mu) - \frac{1}{2\mu} \int_0^1 S(\tau_1; \mu, \mu') I_P(\tau_1, +\mu') d\mu' \\
 - e^{-\tau_1/\mu} I_P(0, -\mu) - \frac{1}{2\mu} \int_0^1 T(\tau_1; \mu, \mu') I_P(0, -\mu') d\mu',
 \end{aligned} \tag{2}$$

where

$$I(0, -\mu) = I(\tau_1, +\mu) \equiv 0 \quad (0 < \mu \leq 1), \tag{3}$$

and where  $S$  and  $T$  are the diffuse scattering and transmission functions in Chandrasekhar's (1950) notation for atmospheres of normal optical thickness  $\tau_1$ . Physically equations (1) and (2) arise from the fact that any mass element at a level  $\tau$  ( $0 \leq \tau \leq \tau_1$ ) is unable to distinguish between being imbedded in a doubly infinite atmosphere and being imbedded in a finite atmosphere that is irradiated on the top and bottom by the radiation fields  $I_P(0, -\mu)$  and  $I_P(\tau_1, +\mu)$ , respectively.

Consider the equation of transfer for a partially thermally emitting, partially anisotropically scattering plane-parallel atmosphere:

$$\mu \frac{dI(\tau, \mu)}{d\tau} = I(\tau, \mu) - \frac{1}{2} \int_{-1}^{+1} \hat{p}(\tau; \mu, \mu') I(\tau, \mu') d\mu' - (1 - \varpi_0) B(\tau). \quad (4)$$

Let  $\hat{p}(\tau; \mu, \mu') = \hat{p}(\mu, \mu')$  be independent of  $\tau$ . Further let  $\hat{p}(\mu, \mu')$  be the azimuth-independent part of the expansion in spherical harmonics of a finite Legendre polynomial series approximation of the phase function for single scattering, and let  $B(\tau)$  be approximated by a finite power series in  $\tau$ ; i.e.,

$$\hat{p}(\mu, \mu') = \sum_{l=0}^N \varpi_l P_l(\mu) P_l(\mu') \quad (5)$$

and

$$B(\tau) = \sum_{r=0}^M b_r \tau^r. \quad (6)$$

It can be shown (cf. Samuelson 1965) that a particular integral satisfying equation (4) under conditions (5) and (6) is given by

$$I_P(\tau, \mu) = \sum_{r=0}^M \tau^r \sum_{s=r}^M c_{r,s} P_{s-r}(\mu), \quad (7)$$

where the constant coefficients  $c_{r,s}$  are uniquely generated by the recursion relations

$$\left. \begin{aligned} \left[ 1 - \frac{\varpi_{M-r}}{2(M-r)+1} \right] c_{r,M} &= \frac{(r+1)(M-r)}{2(M-r)-1} c_{r+1,M} & (0 \leq r \leq M-1) \\ \left[ 1 - \frac{\varpi_{M-r-1}}{2(M-r)-1} \right] c_{r,M-1} &= \frac{(r+1)(M-r-1)}{2(M-r)-3} c_{r+1,M-1} & (0 \leq r \leq M-2) \\ (1 - \varpi_0)(c_{r,r} - b_r) &= \frac{1}{3}(r+1) c_{r+1,r+2} & (0 \leq r \leq M-2) \\ \left[ 1 - \frac{\varpi_{s-r}}{2(s-r)+1} \right] c_{r,s} &= (r+1) \\ \times \left[ \frac{(s-r+1)}{2(s-r)+3} c_{r+1,s+2} + \frac{(s-r)}{2(s-r)-1} c_{r+1,s} \right] & & \left. \begin{aligned} (0 \leq r \leq M-3) \\ (r+1 \leq s \leq M-2) \end{aligned} \right\} \quad (8) \end{aligned}$$

where

$$c_{M,M} = b_M, \quad c_{M-1,M-1} = b_{M-1}, \quad \varpi_\lambda = 0 \quad (\lambda > N). \quad (9)$$

That equation (7) is also the complete solution for a doubly infinite atmosphere is rendered plausible on physical grounds by noting that (cf. eq. [6])

$$\lim_{\tau \rightarrow \infty} \left[ \frac{1}{2} \int_{-1}^{+1} I_P(\tau, \mu) d\mu \right] = \lim_{\tau \rightarrow \infty} [B(\tau)] \quad (10)$$

and

$$\lim_{\tau \rightarrow \infty} \left[ 2\pi \int_{-1}^{+1} \mu I_P(\tau, \mu) d\mu \right] = \frac{4\pi}{3 - \varpi_1} \lim_{\tau \rightarrow \infty} \left[ \frac{dB(\tau)}{d\tau} \right]; \quad (11)$$

i.e., the limiting values of the average specific intensity and the net flux are, respectively, equal to and proportional to the limiting values of the Planck function and its divergence.

Now Chandrasekhar's  $\psi$ - and  $\phi$ -functions of order zero and degree  $l$  are defined by (Chandrasekhar 1950)

$$\psi_l(\tau_1; \mu) = P_l(\mu) + \frac{(-1)^l}{2} \int_0^1 S(\tau_1; \mu, \mu') P_l(\mu') \frac{d\mu'}{\mu'} \quad (12)$$

and

$$\phi_l(\tau_1; \mu) = e^{-\tau_1/\mu} P_l(\mu) + \frac{1}{2} \int_0^1 T(\tau_1; \mu, \mu') P_l(\mu') \frac{d\mu'}{\mu'}. \quad (13)$$

Upon multiplying through both numerator and denominator in all the integrands of equations (1) and (2) by  $\mu'$ , it can be readily demonstrated, with the aid of equations (7), (12), and (13) and the relation

$$(2l+1)\mu P_l(\mu) = (l+1)P_{l+1}(\mu) + lP_{l-1}(\mu), \quad (14)$$

that equations (1) and (2), respectively, reduce to

$$I(0, +\mu) = \frac{1}{\mu} \sum_{s=0}^M \frac{c_{0,s}}{2s+1} [(s+1)\psi_{s+1}(\tau_1; \mu) + s\psi_{s-1}(\tau_1; \mu)] \\ - \frac{1}{\mu} \sum_{r=0}^M \tau_1^r \sum_{s=r}^M \frac{c_{r,s}}{2(s-r)+1} [(s-r+1)\phi_{s-r+1}(\tau_1; \mu) + (s-r)\phi_{s-r-1}(\tau_1; \mu)] \quad (15)$$

and

$$I(\tau_1, -\mu) = \frac{1}{\mu} \sum_{r=0}^M \tau_1^r \sum_{s=r}^M \frac{(-1)^{s-r} c_{r,s}}{2(s-r)+1} \\ \times [(s-r+1)\psi_{s-r+1}(\tau_1; \mu) + (s-r)\psi_{s-r-1}(\tau_1; \mu)] \\ - \frac{1}{\mu} \sum_{s=0}^M \frac{(-1)^s c_{0,s}}{2s+1} [(s+1)\phi_{s+1}(\tau_1; \mu) + s\phi_{s-1}(\tau_1; \mu)], \quad (16)$$

where all  $\psi$ 's and  $\phi$ 's of negative degree are defined to be bounded in the interval ( $0 \leq \mu \leq 1$ ).

Equations (15) and (16) are notable in two respects. First, the only non-elementary functions involved are the  $\psi$ - and  $\phi$ -functions of zero order. For a given  $\tau_1$  and set of  $\varpi_l (l = 0, \dots, N)$  (cf. also eq. [9]) these functions may be calculated once and for all with the aid of existing computer programs (cf. Churchill, Chu, Evans, Tien, and Pang 1961). And second, the complete description of the thermal properties of the atmosphere is contained entirely in the constant coefficients  $c_{r,s} (r = 0, \dots, M; s = r, \dots, M)$ . In view of the foregoing remarks and the simplicity of relations (8), the practical problem of solving equations (15) and (16) numerically should not be inordinately difficult. The additional problem of calculating the planetary limb darkening under restrictions (5) and (6) in accordance with Chandrasekhar's discussion of the "planetary problem" is quite straightforward.

Some question might be raised about the validity of approximations (5) and (6) in the context of real planetary atmospheres. In order to test the usefulness of equation (5), the Mie theory was used to compute the phase function for single scattering  $p(\cos \Theta)$  for a flat particle-diameter range ( $0 \leq d \leq 12.73$  microns) and for a wavelength of thermal radiation  $\lambda = 10$  microns. Computations were made for eighteen separate complex indices of refraction covering the range ( $1.10 - 0.01i \leq \bar{n} \leq 1.60 - 0.50i$ ). It was found that the shape of  $p(\cos \Theta)$  is almost independent of  $\bar{n}$ ; hence, the arithmetic

average of the eighteen phase functions, illustrated in Figure 1, should be quite representative of various substances for the particle-size distribution considered. It was found that setting  $N = 13$  in equation (5) would allow a least-squares fit of  $p(\cos \Theta)$  which was nowhere in error by more than 0.3 per cent; the maximum relative error over the forward scattering lobe was less than 0.1 per cent. Increasing the maximum particle size to  $d = 19$  microns increased the maximum relative error in  $p(\cos \Theta)$  to about 1.0 per cent for the same value of  $N$ . Larger particle diameters caused the errors to grow rapidly. In any event equation (5) appears to approximate many realistic phase functions quite well for reasonable values of  $N$ .

Equation (6) should be an excellent approximation to the Planck function for small optical thicknesses. As  $\tau_1 \rightarrow \infty$ , however, it is clear that equation (6) may have severe limitations due to the requirement that  $M$  be finite. The critical question is whether or not the rapid departure of equation (6) from the exact Planck function at large optical

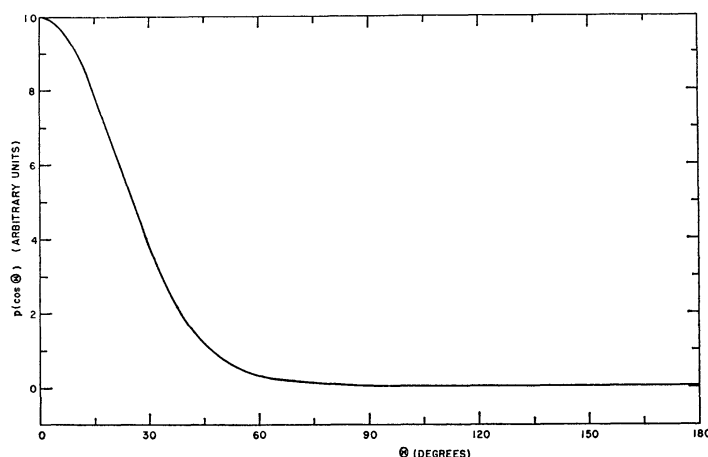


FIG. 1.—Phase function for single scattering representative of a flat particle-size distribution covering the range  $(0 \leq d \leq 12.73$  microns). The wavelength of radiation is taken to be  $\lambda = 10$  microns.

depths (going roughly as  $\tau^M$ ) can be compensated adequately by the exponential attenuation of the corresponding radiation field generated at  $\tau$  as it diffuses to the top of the atmosphere. In other words, does the formal solution to equation (4),

$$I(0, \mu) = \int_0^\infty \mathcal{J}(\tau, \mu) e^{-\tau/\mu} \frac{d\tau}{\mu}, \quad (17)$$

where  $\mathcal{J}(\tau, \mu)$  is the source function, depend critically on the choice for the formal representation of  $B(\tau)$ ?

In the extreme case of complete forward scattering [ $p(\cos \Theta) = 0$  for  $\Theta \neq 0$ ] equation (17) may be replaced with

$$I(0, \mu) = \int_0^\infty B(\tau) e^{-t/\mu} \frac{dt}{\mu}, \quad (18)$$

where  $t = (1 - \omega_0)\tau$  is the effective optical depth arising from absorption alone. Substituting in equation (18) according to equation (6) we obtain

$$\sum_{r=0}^M b_r r! \left( \frac{\mu}{1 - \omega_0} \right)^r \simeq \sum_{j=1}^m a_j B \left( \frac{\mu x_j}{1 - \omega_0} \right), \quad (19)$$

where the right-hand side of expression (19) is a quadrature formula for equation (18) based on the zeros  $x_j$  of the Laguerre polynomials  $L_m(x)$  (Chandrasekhar 1950, pp. 64–65); the  $a_j$ 's are the corresponding Christoffel numbers. Equation (19) may be solved for  $b_r$  ( $r = 0, \dots, M$ ) by selecting appropriate values for  $\mu$ . In practice, of course, scattering plays an important role in describing the rate of attenuation of the radiation field as it diffuses outward. Hence in general expression (19) weights  $B(\tau)$  too heavily at large optical depths. On the other hand expression (19) will assure a sufficient consideration of  $B(\tau)$  at large  $\tau$  for all forms of scattering.

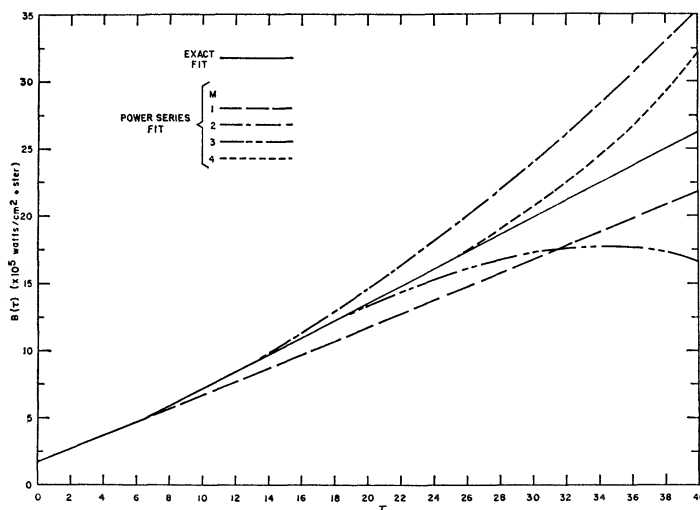


FIG. 2.—The Planck function for the model atmosphere described in the text. The exact function is indicated by the solid curve, while the four power series approximations to this curve are computed in accordance with eqs. (6) and (19).

TABLE 1  
OUTGOING INTENSITIES  $I(0, \mu)$  IN UNITS OF  $F$

$\mu$	$M=1$	$M=2$	$M=3$	$M=4$
0 986284 . . . . .	1.17258	1 17550	1.17665	1.17662
928435 . . . . .	1 14362	1 14540	1 14628	1 14628
.827201 . . . . .	1.09217	1.09239	1.09282	1 09284
.687293 . . . . .	1 01861	1 01753	1 01740	1 01743
515249 . . . . .	0 92142	0 91997	0 91933	0 91933
319112 . . . . .	0 79405	0 79354	0 79266	0 79262
0 108055 . . . . .	0 61705	0 61842	0 61773	0 61768
$F (10^{-5} \text{ watts/cm}^2) . .$	2 38303	2 36041	2 36263	2 36276

With the adoption of expression (19) the efficacy of equation (6) can best be demonstrated with the solution of equation (4) for a physically realistic model atmosphere. The model adopted for this purpose was prescribed a temperature at the top of  $T_c = 220^\circ \text{K}$ , and an adiabatic lapse rate of  $-(dT/dz) = 8.6^\circ \text{K/km}$ . The particle density  $N_0$  was taken to be 10 particles/cm<sup>3</sup> at the top and allowed to increase in direct proportion to the atmospheric density as the geometrical height  $z$  decreases. The phase function for single scattering adopted was that of Figure 1, normalized to  $\omega_0 = 0.7$ . From calculations in accordance with the Mie theory it was found that an effective cross-section per particle for the particle-size distribution corresponding to  $p(\cos \Theta)$  in Figure 1 is quite

well represented by  $\chi_E = 10^{-6}$  cm<sup>2</sup>/particle, yielding an effective extinction coefficient  $N_0\chi_E = 10^{-5}$  cm<sup>-1</sup> at  $\tau = 0$ .

Equation (4) was solved for this model by the method of discrete ordinates in the seventh approximation (Chandrasekhar 1950; cf. also Samuelson [1965] for extending the method to include the particular integral [7]). Equation (5) was used with  $N = 13$  and equation (6) considered for the four cases  $M = 1, 2, 3,$  and  $4$ , while expression (19) was solved in all cases with  $m = 5$ . In practice it was found best to anchor  $B(\tau)$  at the top of the atmosphere—i.e., preassign the value of  $b_0$ . The functional dependence of  $B(\tau)$  on  $\tau$  is shown in Figure 2 for the exact model as well as for the four power series approximations, while the outgoing intensities  $I(0, \mu_i)$  ( $i = 1, \dots, 7$ ) are tabulated in units

TABLE 2  
OUTGOING INTENSITIES  $I(0, \mu)$  CONVERTED TO TEMPERATURE ( $^{\circ}$  K)

$\mu$	$M=1$	$M=2$	$M=3$	$M=4$
0 986284	237 40	237 12	237 20	237 20
928435	236 43	236 12	236 18	236 19
827201	234 66	234 30	234 35	234 35
687293 . .	232 02	231 62	231 66	231.66
515249	228 33	227 93	227 94	227 94
319112	223 07	222 72	222 72	222 72
0 108055	214 68	214 45	214 45	214 45
$T_E$ ( $^{\circ}$ K)	231 33	230 98	231 01	231 02

of  $F(\pi F =$  the net outgoing flux) in Table 1 and converted to units of temperature in Table 2. Also included in Table 2 are the effective temperatures  $T_E$ . All computations were performed over the wavenumber interval ( $995 \text{ cm}^{-1} \leq \nu \leq 1005 \text{ cm}^{-1}$ ).

The agreement among the intensities and temperatures in the tables is excellent, especially for  $M = 3$  and  $4$ , in spite of the fact that the representations for  $B(\tau)$  in Figure 2 are quite different. Since the difference  $T_E - T_c$  is on the order of  $+11^{\circ}$  K, it is clear that  $B(\tau)$  plays an important role. It can only be concluded that equation (6) is in fact quite adequate for approximating the Planck function successfully in many realistic problems. From the above discussion it would seem that the exact solutions to the standard problem given by equations (15) and (16) hold considerable promise from the practical point of view.

R. E. SAMUELSON

March 31, 1966; revised August 18, 1966  
GODDARD SPACE FLIGHT CENTER  
GREENBELT, MARYLAND

#### REFERENCES

- Chandrasekhar, S 1950, *Radiative Transfer* (Oxford: Clarendon Press), pp. 92; 177–180; Appendix III, pp 383–385.  
Churchill, S., Chu, C., Evans, L., Tien, L., and Pang, S. 1961, *U. of Mich. Rept DASA-1257* (Ann Arbor: University of Michigan).  
Goody, R. 1964, *Icarus*, **3**, 98.  
Mullikin, T. W. 1962, *RAND Mem. RM-3209-NASA* (Santa Monica, Calif : RAND Corporation), p 87.  
Murray, B. C , Wildey, R. L , and Westphal, J. A. 1963, *J. Geophys. Res.*, **68**, 4813.  
———. 1964, *Ap. J.*, **139**, 986  
Pollack, J. B., and Sagan, C. 1965, *J. Geophys. Res* , **70**, 4403  
Samuelson, R. E. 1965, *NASA Tech. Rept R-215* (Washington, D C.: National Aeronautics and Space Administration), Appendix B, pp 61–67.  
Westphal, J. A., Wildey, R. L., and Murray, B. C. 1965, *Ap J.*, **142**, 799.

ON THE FORMULAE FOR CHANDRASEKHAR'S  $X$ - AND  
 $Y$ -FUNCTIONS IN THICK ATMOSPHERES\*

The evaluation of Chandrasekhar's  $X$ - and  $Y$ -functions for homogeneous atmospheres of large thickness ( $\tau_0 \gg 1$ ) has recently received considerable attention. Bellman, Kagiwada, Kalaba, and Ueno (1965) and Mullikin (1964) have obtained series expansions useful for computational purposes. For large  $\tau_0$ , however, asymptotic analytic formulae give more insight concerning the behavior of  $X$  and  $Y$ . In the case of isotropic scattering, these formulae take the form

$$X(\mu) = H(\mu)(1 - k\mu)^{-1}[1 - k\mu \coth k(\tau_0 + 2z_0)] + O(e^{-\tau_0}), \quad (1)$$

$$Y(\mu) = H(\mu)(1 - k\mu)^{-1}[k\mu \operatorname{csch} k(\tau_0 + 2z_0)] + O(e^{-\tau_0}), \quad (2)$$

where  $0 \leq \mu \leq 1$ . Here  $H(\mu)$  is the  $H$ -function of Chandrasekhar (1950) for isotropic scattering and  $k$  is the positive root of the characteristic equation

$$1 = \frac{\varpi_0}{2k} \ln \left[ \frac{1+k}{1-k} \right].$$

The constant  $\varpi_0$  is the albedo for a single scattering and  $z_0$  is the Milne extrapolation distance tabulated by Case, de Hoffmann, and Placzek (1953). The product  $\varpi_0 z_0$  monotonically decreases from 1 at  $\varpi_0 = 0$  to 0.710446 . . . at  $\varpi_0 = 1$  and then monotonically increases to  $\frac{3}{4}$  at  $\varpi_0 = \infty$ . In the limit of no absorption ( $\varpi_0 \rightarrow 1$ ), equations (1) and (2) reduce to

$$X(\mu) = H(\mu)[1 - \mu(\tau_0 + 2z_0)^{-1}] + O(e^{-\tau_0}), \quad (3)$$

$$Y(\mu) = H(\mu)[\mu(\tau_0 + 2z_0)^{-1}] + O(e^{-\tau_0}), \quad (4)$$

whereas for a purely absorbing medium ( $\varpi_0 \rightarrow 0$ ) they become

$$X(\mu) = 1 + O(e^{-\tau_0}), \quad (5)$$

$$Y(\mu) = O(e^{-\tau_0}). \quad (6)$$

Equations (1) and (2) are valid for  $0 < \varpi_0 < 1$  and can be obtained by four independent approaches. The easiest involves the observation that, for isotropic scattering,  $X(\mu)$  and  $Y(\mu)$  are the average intensities (radiation densities) on the surfaces of a finite slab irradiated by an incident parallel beam of radiation in the direction  $\mu$  (Chandrasekhar 1950, § 62.1). These asymptotic average intensities are immediately written down in the above form using the results of Kušćer (1953).

The two equations, together with an estimate of the terms  $O(e^{-\tau_0})$ , may also be obtained by utilizing the lowest-order results of a singular eigenfunction analysis of the problem of diffuse reflection and transmission by plane-parallel atmospheres (McCormick and Mendelson 1964).

The results published by Sobolev (1964, eqs. [29] and [30]) agree exactly with equations (1) and (2) except for our use of the tabulated Milne extrapolation distance instead of integrals involving  $k$  and  $H(\mu)$ . This alternate form of expressing the  $X$  and  $Y$  for large  $\tau_0$  removes the difficulties encountered by Heaslet and Warming (1965) when using Sobolev's results.

Finally, equations (1) and (2) may be obtained directly from the asymptotic relations given by Carlstedt and Mullikin (1966, eq. [4.4] and [4.5]) by restricting their  $z$  to  $\mu$ ,  $0 \leq \mu \leq 1$ . In terms of their tabulated functions,

$$z_0 = \frac{1}{2k} \ln \left[ -\frac{N(1/k)}{N(-1/k)} \right]. \quad (7)$$

\* Based in part upon a Ph.D. thesis at the University of Michigan, 1965.

If the values of  $X$  and  $Y$  for argument  $0 \leq \mu \leq 1$  are desired, the form of equations (1) and (2) is perhaps preferable to that of other formulae previously published since it gives the results in terms of the easily visualized parameter  $z_0$ . It should be noted, however, that for other values of the argument of  $X$  and  $Y$  the asymptotic forms of Carlstedt and Mullikin should be used since the first terms in the right-hand sides of equations (1) and (2) have a pole at  $1/k$ . The formulae given by them seem to be the first which (correctly) do not have poles at  $1/k$ .

The derivation of equations (3) and (4) follows in a straightforward manner from equations (1) and (2) (Sobolev 1964). The results are those reported previously by Sobolev (1956, 1957, 1964) and van de Hulst (1964). Equations (5) and (6) can be obtained from equations (1) and (2) by using the expansion in terms of  $\varpi_0$  for  $k$  near unity (Case *et al.* 1953). Since the extrapolation distance adequately compensates for the nearness of the pole in equations (1) and (2), the results are in obvious agreement with those obtained by allowing  $\varpi_0 \rightarrow 0$  in the definitions of  $X$  and  $Y$ . Note that equation (2) is not a satisfactory asymptotic expansion for large absorption, its particular range of usefulness depending upon  $\mu$ ,  $\varpi_0$ , and  $\tau_0$ .

Equations (1)–(4) may be used to give asymptotic values for the moments  $x_n$  and  $y_n$  in terms of  $h_n(\varpi_0 a_n/2$  in Chandrasekhar's notation). For non-conservative scattering ( $0 < k < 1$ ), we find

$$x_0 = 1 - (1 - h_0) \coth k(\tau_0 + 2z_0) + O(e^{-\tau_0}), \quad (8)$$

$$k^n x_n = 1 - \sum_{i=0}^{n-1} k^i h_i - \left(1 - \sum_{i=0}^n k^i h_i\right) \coth k(\tau_0 + 2z_0) + O(e^{-\tau_0}), \quad n \geq 1, \quad (9)$$

$$k^n y_n = \left(1 - \sum_{i=0}^n k^i h_i\right) \operatorname{csch} k(\tau_0 + 2z_0) + O(e^{-\tau_0}), \quad n \geq 0. \quad (10)$$

For conservative scattering ( $k = 0$ ) we have

$$x_n = h_n - h_{n+1}(\tau_0 + 2z_0)^{-1} + O(e^{-\tau_0}), \quad n \geq 0, \quad (11)$$

$$y_n = h_{n+1}(\tau_0 + 2z_0)^{-1} + O(e^{-\tau_0}), \quad n \geq 0. \quad (12)$$

N. J. McCORMICK

May 18, 1966; revised July 25, 1966  
DEPARTMENT OF NUCLEAR ENGINEERING  
UNIVERSITY OF WASHINGTON  
SEATTLE, WASHINGTON

#### REFERENCES

- Bellman, R. E., Kagiwada, H. H., Kalaba, R. E., and Ueno, S. 1965, *J. Math. Anal. Appl.*, **12**, 541.  
Carlstedt, J. L., and Mullikin, T. W. 1966, *Ap. J. Suppl.*, **12**, 449 (No. 113).  
Case, K. M., Hoffmann, F. de, and Placzek, G. 1953, *Introduction to the Theory of Neutron Diffusion* (Washington, D. C.: Government Printing Office).  
Chandrasekhar, S. 1950, *Radiative Transfer* (Oxford: Clarendon Press).  
Heaslet, M. A., and Warming, R. F. 1965, *J. Quant. Spectrosc. Radiat. Transfer*, **5**, 669.  
Hulst, H. C. van de 1964, *Icarus*, **3**, 336.  
Kuščer, I. 1953, *Canadian J. Phys.*, **31**, 1187.  
McCormick, N. J., and Mendelson, M. R. 1964, *Nucl. Sci. Eng.*, **20**, 462.  
Mullikin, T. W. 1964, *Trans. Am. Math. Soc.*, **113**, 316.  
Sobolev, V. V. 1956, *Radiative Transfer in Stellar and Planetary Atmospheres* (Moscow) (English translation, *A Treatise on Radiative Transfer* [Princeton, N. J.: D. Van Nostrand Co., 1963]).  
———. 1957, *Astr. Zh.*, **34**, 336 (*Soviet Astr.*—*A. J.*, **1**, 332).  
———. 1964, *Dokl. Akad. Nauk SSSR*, **155**, 316 (*Soviet Phys.—Doklady*, **9**, 222).